Correction

MEDICAL SCIENCES

Correction for "Stromal-derived interleukin 6 drives epithelial-to-mesenchymal transition and therapy resistance in esophageal adenocarcinoma," by Eva A. Ebbing, Amber P. van der Zalm, Anne Steins, Aafke Creemers, Simone Hermsen, Rosa Rentenaar, Michelle Klein, Cynthia Waasdorp, Gerrit K. J. Hooijer, Sybren L. Meijer, Kausilia K. Krishnadath, Cornelis J. A. Punt, Mark I. van Berge Henegouwen, Suzanne S. Gisbertz, Otto M. van Delden, Maarten C. C. M. Hulshof, Jan Paul Medema, Hanneke W. M. van Laarhoven, and Maarten F. Bijlsma, which was first published January 22, 2019; 10.1073/pnas.1820459116 (*Proc. Natl. Acad. Sci. U.S.A.* **116**, 2237–2242).

The authors note that Fig. 3 appeared incorrectly. "The authors would like to note that in Fig. 3*B*, the untreated (control) 031M organoids and those of the 081RF sup + a-IL-6 condition showed duplicate images at different exposures." The corrected figure and its legend appear below. The online version has been corrected.

CORRECTION

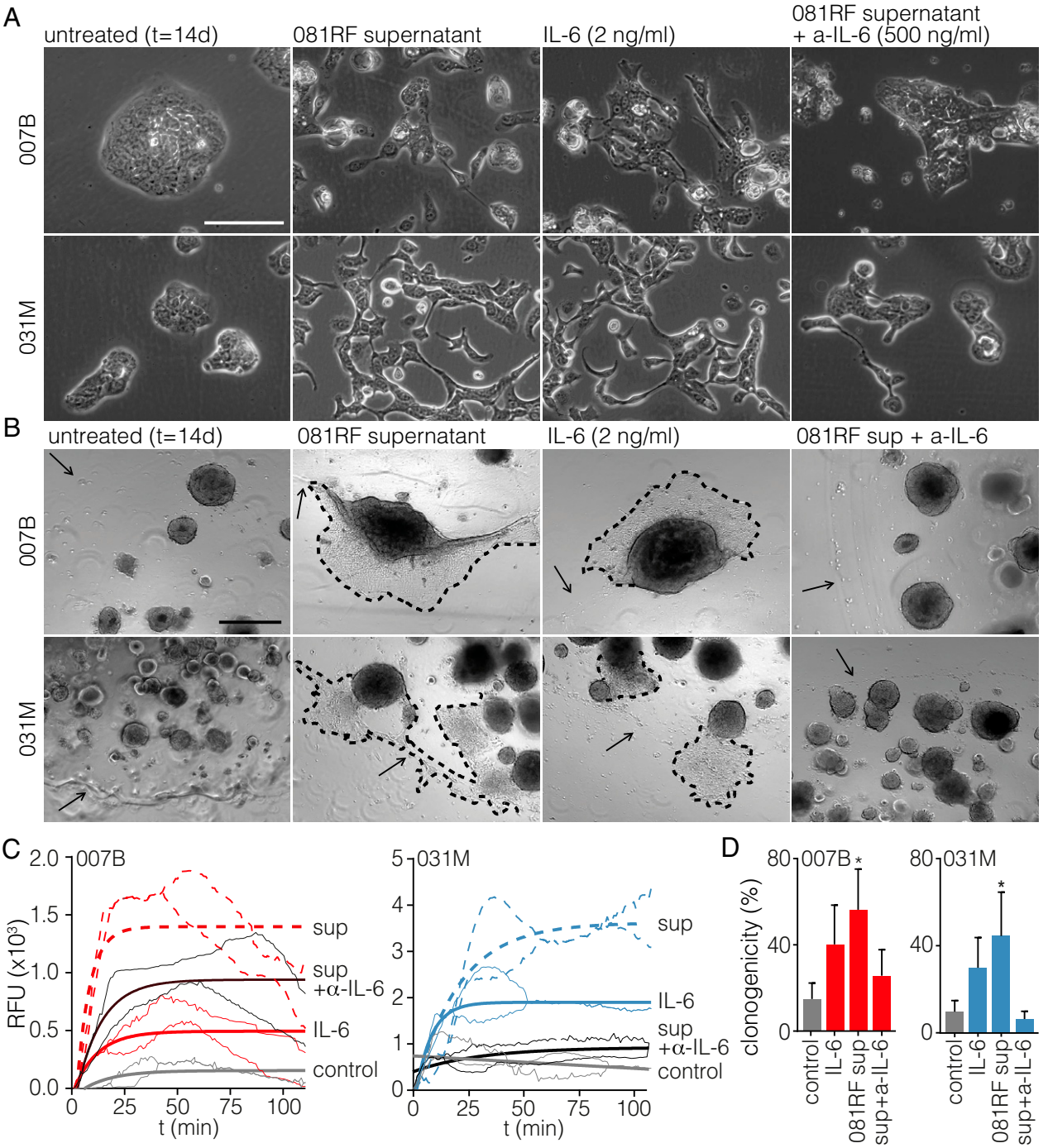

Fig. 3. CAF-secreted IL-6 induces epithelial-to-mesenchymal transition. (*A*) The 007B and 031M cultures were exposed to the following conditions for 14 d: unconditioned medium (untreated), 081RF supernatant (1 in 4 diluted), recombinant IL-6, and 081RF + IL-6–neutralizing antibody. Morphology was assessed by phase-contrast microscopy. (Scale bar: 200 μm.) (*B*) As for *A* using 007B and 031M organoid cultures. Dashed lines indicate the migratory front of cells migrating out of the organoid. Arrows indicate the edge of the Matrigel cushion. (*C*) Transwell migration assays on 007B and 031M cells cultured for 14 d in the conditions as for *A* before the assay. In the transwell assays, 1% FCS was used as a chemoattractant. Migration shown is corrected for no-attractant controls (medium without FCS), $n = 3$. *P* values were determined by two-way ANOVA and Tukey's multiple comparisons correction, one-phase exponential curves were fitted, and the lines of matching color indicate the SD. (*D*) Limiting dilution assays were performed using 007B and 031M cells after incubation for 14 d in the indicated conditions. Cells were sorted into 96-well plates. Bar graphs show means ± SEM, $n = 3$. *$P < 0.05$, **$P < 0.01$, ***$P < 0.001$, and ****$P < 0.0001$. Significance was tested by two-sided unpaired *t* tests compared with the control.

Published August 31, 2021.

www.pnas.org/cgi/doi/10.1073/pnas.2113728118

Stromal-derived interleukin 6 drives epithelial-to-mesenchymal transition and therapy resistance in esophageal adenocarcinoma

Eva A. Ebbing[a,b,1], Amber P. van der Zalm[a,c,1], Anne Steins[a,b,c], Aafke Creemers[a,b], Simone Hermsen[a,b], Rosa Rentenaar[a,b], Michelle Klein[a,b], Cynthia Waasdorp[a,c], Gerrit K. J. Hooijer[d], Sybren L. Meijer[d], Kausilia K. Krishnadath[a,e], Cornelis J. A. Punt[b], Mark I. van Berge Henegouwen[f], Suzanne S. Gisbertz[f], Otto M. van Delden[g], Maarten C. C. M. Hulshof[h], Jan Paul Medema[a,c], Hanneke W. M. van Laarhoven[b,2], and Maarten F. Bijlsma[a,c,2,3]

[a]Laboratory for Experimental Oncology and Radiobiology, Center for Experimental and Molecular Medicine, Amsterdam UMC, University of Amsterdam, Cancer Center Amsterdam, 1105 AZ Amsterdam, The Netherlands; [b]Department of Medical Oncology, Amsterdam UMC, University of Amsterdam, Cancer Center Amsterdam, 1105 AZ Amsterdam, The Netherlands; [c]Oncode Institute, Amsterdam UMC, 1105 AZ Amsterdam, The Netherlands; [d]Department of Pathology, Amsterdam UMC, University of Amsterdam, Cancer Center Amsterdam, 1105 AZ Amsterdam, The Netherlands; [e]Department of Gastroenterology and Hepatology, Amsterdam UMC, University of Amsterdam, Cancer Center Amsterdam, 1105 AZ Amsterdam, The Netherlands; [f]Department of Surgery, Amsterdam UMC, University of Amsterdam, Cancer Center Amsterdam, 1105 AZ Amsterdam, The Netherlands; [g]Department of Radiology, Amsterdam UMC, University of Amsterdam, Cancer Center Amsterdam, 1105 AZ Amsterdam, The Netherlands; and [h]Department of Radiotherapy, Amsterdam UMC, University of Amsterdam, Cancer Center Amsterdam, 1105 AZ Amsterdam, The Netherlands

Edited by Tadamitsu Kishimoto, Laboratory of Immune Regulation, World Premier Immunology Frontier Research Centre, Osaka University, Suita, Japan, and approved December 19, 2018 (received for review December 3, 2018)

Esophageal adenocarcinoma (EAC) has a dismal prognosis, and survival benefits of recent multimodality treatments remain small. Cancer-associated fibroblasts (CAFs) are known to contribute to poor outcome by conferring therapy resistance to various cancer types, but this has not been explored in EAC. Importantly, a targeted strategy to circumvent CAF-induced resistance has yet to be identified. By using EAC patient-derived CAFs, organoid cultures, and xenograft models we identified IL-6 as the stromal driver of therapy resistance in EAC. IL-6 activated epithelial-to-mesenchymal transition in cancer cells, which was accompanied by enhanced treatment resistance, migratory capacity, and clonogenicity. Inhibition of IL-6 restored drug sensitivity in patient-derived organoid cultures and cell lines. Analysis of patient gene expression profiles identified ADAM12 as a noninflammation-related serum-borne marker for IL-6–producing CAFs, and serum levels of this marker predicted unfavorable responses to neoadjuvant chemoradiation in EAC patients. These results demonstrate a stromal contribution to therapy resistance in EAC. This signaling can be targeted to resensitize EAC to therapy, and its activity can be measured using serum-borne markers.

IL-6 | tumor stroma | therapy resistance | esophageal adenocarcinoma | epithelial-to-mesenchymal transition

Esophageal cancer has a poor prognosis and currently ranks sixth in cancer-related mortality (1, 2). A steep increase in the incidence of the esophageal adenocarcinoma (EAC) subtype has been observed in Western countries (2). Patients eligible for curative treatment typically receive neoadjuvant chemoradiation therapy, followed by surgery (3). The efficacy of this regimen is modest, indicating a need to identify the mechanisms that contribute to therapy resistance.

Research on therapy resistance has centered on tumor cell-intrinsic properties, but it is increasingly clear that the tumor microenvironment (TME) is important for this as well (4). Cancer-associated fibroblasts (CAFs) comprise the majority of the TME and are suspected to exert tumor-promoting activities by their mechanical contributions to the stroma, as well as by the secretion of cytokines (5). The presence of CAFs, as determined by expression of smooth muscle actin (α-SMA), is associated with poor survival in many solid malignancies (6–9), but the exact tumor-promoting activities of these cells vary between cancer types (10). The specific contributions of CAFs depend on the cytokines produced.

IL-6 is primarily known for its role in inflammation, which can result from exposure to anticancer drugs and ionizing radiation. IL-6 may also be expressed in the absence of therapeutic stress (11, 12). In various cancer types, both the tumor cells and CAFs can produce IL-6 (13–16). The tumor-promoting activities of IL-6 are manifold and include the evasion of growth suppression by regulating the *TP53* gene (17), mediating resistance against cell death (18, 19), increasing stemness of tumor cells (20, 21), and mediating tumor invasion and metastasis (22–24). Also, stroma-derived IL-6 is dysregulated in the metaplasia–dysplasia–EAC sequence (25).

Surprisingly little is known about the role of CAFs in EAC (8, 9, 26, 27). In this study, tumor cells and EAC-associated fibroblasts were isolated and used to identify a mechanism of resistance against currently applicable treatment regimens in EAC. Stromal IL-6 was identified as the molecule driving this resistance, and targeting IL-6 resulted in resensitization of tumor cells to chemoradiotherapy.

Significance

We found that cancer-associated fibroblasts, the most abundant noncancer cell type in esophageal cancer tissue, contribute to the resistance of tumors against currently applicable treatments. These cancer-associated fibroblasts do so by producing and secreting IL-6. IL-6 induces a mesenchymal, resistant tumor cell state. Inhibition of IL-6 reverted the mesenchymal cell state and resensitized tumor cells to therapy. Serum-borne proxies for the presence of IL-6–producing fibroblasts were identified and found to be predictive for the response to neoadjuvant therapy.

Author contributions: E.A.E., J.P.M., H.W.M.v.L., and M.F.B. designed research; E.A.E., A.P.v.d.Z., A.S., A.C., S.H., R.R., M.K., C.W., G.K.J.H., and M.F.B. performed research; S.L.M., K.K.K., C.J.A.P., M.I.v.B.H., S.S.G., O.M.v.D., and M.C.C.M.H. contributed new reagents/analytic tools; E.A.E., A.P.v.d.Z., A.S., A.C., S.L.M., H.W.M.v.L., and M.F.B. analyzed data; H.W.M.v.L. and M.F.B. supervised the project; and E.A.E., A.P.v.d.Z., and M.F.B. wrote the paper.

Conflict of interest statement: M.F.B. has received research funding from Celgene. H.W.M.v.L. has acted as a consultant for Celgene, Eli Lilly and Company, Nordic Pharma Group, and Philips and has received research grants from Amgen, Bayer Schering Pharma AG, Celgene, Eli Lilly and Company, GlaxoSmithKline Pharmaceuticals, Nordic Pharma Group, Philips, and Roche Pharmaceuticals. None were involved in drafting the manuscript.

This article is a PNAS Direct Submission.

[1]E.A.E. and A.P.v.d.Z. contributed equally to this work.

[2]H.W.M.v.L. and M.F.B. contributed equally to this work.

[3]To whom correspondence should be addressed. Email: m.f.bijlsma@amc.uva.nl.

This article contains supporting information online at www.pnas.org/lookup/suppl/doi:10.1073/pnas.1820459116/-/DCSupplemental.

Published online January 22, 2019.

Results

Patient-Derived EAC-Associated Fibroblasts Confer Resistance to Chemotherapy and Radiotherapy. To investigate a possible contribution of CAFs to resistance against conventional chemotherapy and radiation therapy, primary EAC-associated fibroblasts were isolated from resected specimens from patients who received paclitaxel with carboplatin and radiation [the ChemoRadiotherapy for Oesophageal cancer followed by Surgery Study (CROSS) regimen] (3) (*SI Appendix*, Fig. S1*A*). Cells were stained with anti–α-SMA to confirm their activated myofibroblast-like state (*SI Appendix*, Fig. S1*B*). Neoadjuvant chemoradiation is the standard of care in many western European countries and the United States. Therefore, CAFs derived from resection specimens will often have been exposed to this treatment. Two previously established EAC cell lines, OE19 and OE33, were treated with carboplatin, paclitaxel, or radiation in the absence or presence of CAF supernatant. CAF supernatant was found to confer resistance against the applied therapeutics (Fig. 1 *A* and *B*), as well as other clinically relevant agents such as 5-fluorouracil (5-FU), cisplatin, and eribulin (*SI Appendix*, Fig. S1 *C* and *D*). Of note, cells that survived the therapy showed a shift in morphology (Fig. 1*C*). Tumor cell sensitivity to chemotherapeutics was not influenced by the addition of Iscove's Modified Dulbecco's Medium (IMDM) (CAF) medium (*SI Appendix*, Fig. S1 *E* and *F*).

Using mouse CAFs derived from patient-derived xenografts (PDXs), no protective effect was observed (*SI Appendix*, Fig. S2). These results show that EAC-associated fibroblasts confer resistance by secretion of a molecule that harbors species-specific activity.

To ascertain that the CAF-induced resistance is conserved across different EAC cultures, experiments were performed using the supernatant of EAC CAFs isolated from different patients. All conferred resistance to therapy (*SI Appendix*, Fig. S3). To determine if the weight of the molecule conferring resistance falls within the range at which most proteins exist, CAF supernatant was filtered using 10- and 100-kDa filters. This revealed that the chemoprotective effect was lost from 10-kDa filtered supernatant and that it was retained after 100-kDa filtration (Fig. 1*D*). Having established that the candidate molecule is likely a protein, a cytokine array was used to identify it. This revealed IL-6, chemokine ligand 2 (CCL2), and hepatocyte growth factor (HGF) to be the three most abundantly CAF secreted factors (*SI Appendix*, Fig. S4). Cytokine analysis of mouse CAF (isolated from PDXs) supernatant revealed high expression of the same cytokines (*SI Appendix*, Fig. S5).

Stromal CAF-Secreted IL-6 Drives Therapy Resistance. To assess the association of the candidate cytokines with patient outcome, we performed survival analysis on the publicly available TCGA gene expression set containing nonpretreated resected esophageal cancer specimens (28). Samples from EAC (TCGA-EAC) patients were dichotomized by median *IL6*, *CCL2,* or *HGF* expression. A significant association with survival was found for only *IL6* (*SI Appendix*, Fig. S6*A*). To functionally address which cytokine was responsible for the CAF-induced treatment resistance, recombinant IL-6, CCL2, HGF, or CAF supernatant preincubated with the pertinent neutralizing antibodies was used in cell viability assays on two primary EAC cultures receiving carboplatin, paclitaxel, or radiation (Fig. 2 *A*–*F*). Of the candidates tested, IL-6 most consistently affected therapy resistance.

Next, we examined whether IL-6 was specifically produced by CAFs rather than by tumor cells. Indeed, ELISA on cell supernatants showed that IL-6 secretion was restricted to the CAFs and absent from tumor cell cultures (Fig. 2*G*). The 081RF CAFs were derived from patients treated with neoadjuvant chemoradiation therapy. To examine if IL-6 secretion is limited to treated CAFs, we queried public gene expression data from pretreatment EAC biopsies and healthy tissue (29) and found that *IL6* was also significantly higher expressed in untreated cancerous tissue compared with normal tissue (*SI Appendix*, Fig. S6*B*). Gene expression analysis of CAFs isolated from esophageal biopsies revealed these cells to be the likely cellular source of IL-6 in both treated and treatment-naive tissues (*SI Appendix*, Fig. S6*C*) (25). Next, we isolated treatment-naive CAFs from biopsies (117BF, 289BF) and found that these also secreted high amounts of IL-6 (Fig. 2*G*). High IL-6 levels were also found in mouse CAF (031MF) supernatant, further supporting the notion that IL-6 production is not unique to fibroblasts exposed to neoadjuvant chemoradiation (Fig. 2*H*; cocultures with 031M tumor cells also shown).

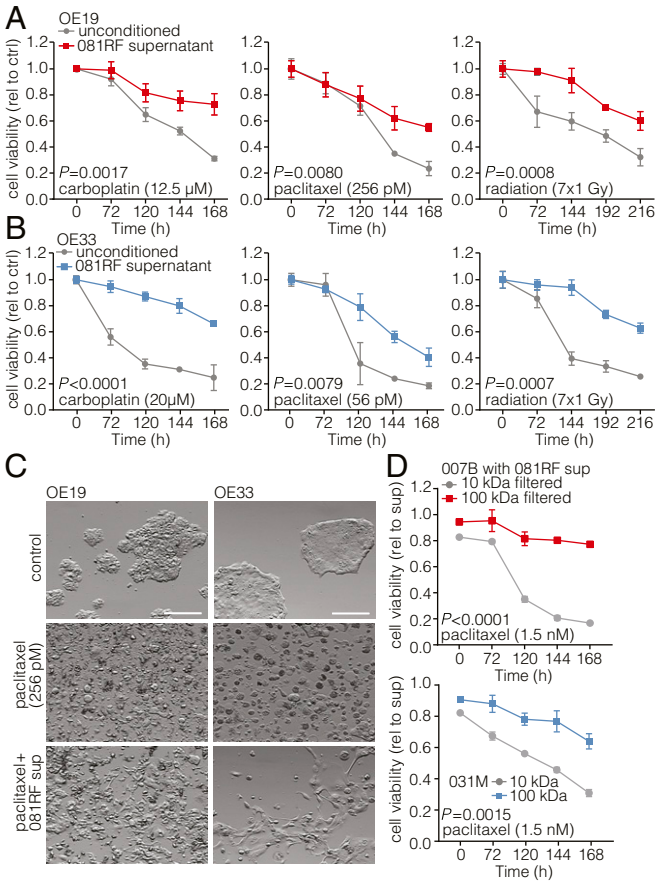

Fig. 1. Patient-derived EAC-associated fibroblasts confer resistance to chemotherapy and radiotherapy. (*A*) Cell viability assays were performed and measured at the indicated times, using OE19 cells incubated with the indicated chemotherapeutics and parenthesized concentrations in unconditioned control (ctrl) medium (gray lines) or medium supplemented with 081RF supernatant (1 in 4 diluted) (colored lines). Graphs show means ± SEM of data normalized to $t = 0$, $n = 3$. *P* values were determined by two-way ANOVA and Bonferroni correction. (*B*) Same as for *A*, using the OE33 cell line. (*C*) OE19 and OE33 cell lines were cultured in unconditioned or 081RF supernatant-supplemented medium (081RF sup), treated with 256 pM paclitaxel or control for 168 h, and morphology was assessed by phase-contrast microscopy. (Scale bar: 100 μm.) (*D*) Cell viability was determined on 007B and 031M cultures which were incubated with 1.5 nM paclitaxel supplemented with 25% 10- or 100-kDa filtered 081RF supernatant. Graphs show means ± SEM, normalized to $t = 0$, $n = 3$. *P* values were determined by two-way ANOVA and Bonferroni correction.

To investigate whether IL-6 secreted by CAFs can activate its canonical pathway in the cancer cells, 007B and 031M cells were stimulated with CAF supernatant, which resulted in STAT3 phosphorylation. The specificity of this effect was confirmed using IL-6–neutralizing antibody (Fig. 2*I*). See *SI Appendix*, Fig. S7 for full membranes. These data suggest that the tumor-promoting properties of the EAC stroma are largely driven by CAF-secreted, biologically active IL-6.

CAF-Derived IL-6 Induces Epithelial-to-Mesenchymal Transition. From the cell viability experiments, a marked change in morphology in the surviving cells was apparent (see Fig. 1*C*). To identify the

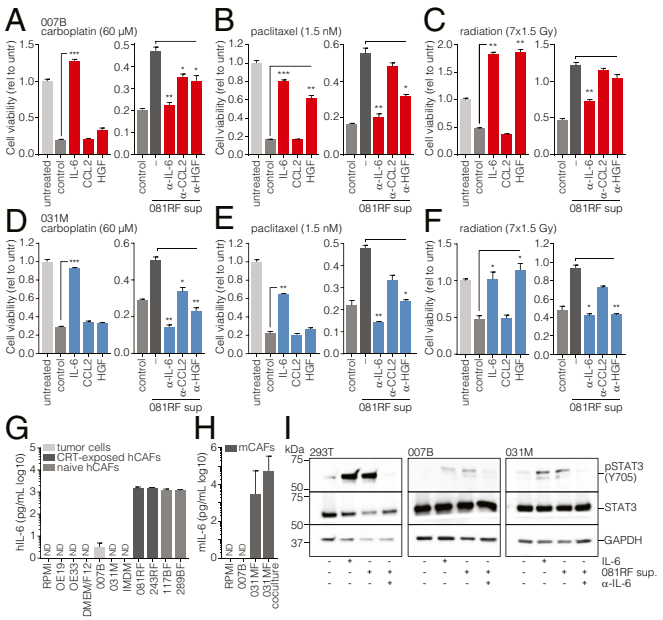

Fig. 2. Stromal CAF-secreted IL-6 drives therapy resistance. (*A–C*) Cell viability assays were performed on primary 007B cells incubated for 168 h in the following culture conditions: unconditioned medium without chemotherapeutics (untreated, untr), unconditioned medium with chemotherapeutics (control), conditioned medium with chemotherapeutics, medium supplemented with the indicated cytokines and chemotherapeutics (colored bars), or 081RF supernatant with or without neutralizing antibodies for the indicated cytokines and chemotherapeutics. Graphs show means ± SEM of data normalized to $t = 0$, $n = 3$. *P* values were by one-way ANOVA and compared with the control or 081RF (–) sup only condition. (*D–F*) As for *A–C*, using 031M cells. (*G*) Human IL-6 was measured by ELISA in 3 d-incubated supernatant of the indicated cultures (5 d for 243RF culture) and media not incubated on cells. (*H*) Mouse IL-6 was measured by ELISA as for *G* in supernatants from indicated (co)cultures. (*I*) 293T, 007B, and 031M cells were stimulated for 20 min with medium containing 081RF supernatant incubated for 3 d, diluted 1 in 4. Recombinant IL-6 was used as a positive control, and IL-6–neutralizing antibody was used as a negative control for IL-6–induced STAT3 phosphorylation. Following exposure, cells were lysed and processed for Western blot analysis for the indicated antigens. $*P < 0.05$, $**P < 0.01$, and $***P < 0.001$.

events responsible for this, we performed gene set enrichment analysis (GSEA) on the TCGA-EAC dataset using gene sets for biological programs associated with such phenotypic transitions. Samples were dichotomized by median *IL6* expression, and a significant association was found for a merged set of two previously published epithelial-to-mesenchymal transition (EMT) signatures and for a stromal infiltration gene set. Additionally, low-*IL6*-expressing tumors associated with an epithelial signature (*SI Appendix*, Fig. S6 *D–F*).

To further ascertain EMT as the mechanism responsible for IL-6–induced therapy resistance, primary cells were cultured with CAF supernatant, IL-6, or CAF supernatant preincubated with IL-6–neutralizing antibody, and morphology was monitored by microscopy. The induction of a mesenchymal morphology was apparent (Fig. 3*A*). These morphological changes were also observed using supernatant from treatment-naive CAFs (*SI Appendix*, Fig. S8). Using early-passage EAC organoids in the same experimental setup, cells in the IL-6–containing conditions were observed to migrate out of the organoid structures and the Matrigel (Fig. 3*B*). To characterize and quantify these observations at the molecular level, EMT markers were measured by transcript analysis, and increased expression of zinc finger E-box-binding homeobox 1 (*ZEB1*), vimentin (*VIM*), snail family transcriptional repressor 2 (*SNAI2*), and *N*-cadherin (*CDH2*) was found in the cultures exposed to IL-6. Epithelial markers E-cadherin (*CDH1*), and cytokeratin 19 (*KRT19*) were decreased (*SI Appendix*, Fig. S9 *A–F*). These changes were confirmed at the protein level by flow cytometry, which showed increased expression of EMT markers C-X-C chemokine receptor type 4 (CXCR4) and VIM and decreased expression of epithelial-related genes human epidermal growth factor receptor 2 (ERBB2), cluster of differentiation 24 (CD24), integrin beta-1 (CD29), and epithelial cell adhesion molecule (EPCAM) (*SI Appendix*, Fig. S9 *E–J*). We and others have previously found human epidermal growth factor receptor 3 (HER3/*ERBB3*) to be a marker for epithelial cell identity, and this protein was also down-regulated following exposure to IL-6 (30–32). Analysis of the kinetics of EMT onset in response to CAF supernatant revealed this EMT to take place within several days, a time frame in line with the induction of chemoresistance (*SI Appendix*, Fig. S10). We take these data to show that IL-6 activates EMT in cancer cells and that this is the mechanism through which resistance against commonly used chemotherapeutics is conferred by the stroma.

IL-6–Induced EMT Is Accompanied by an Enhanced Migratory and Clonogenic Capacity. To study the functional effects of the up-regulated EMT markers in addition to the morphological changes, transwell migration assays were performed, and they showed an enhanced migratory capacity following exposure to IL-6

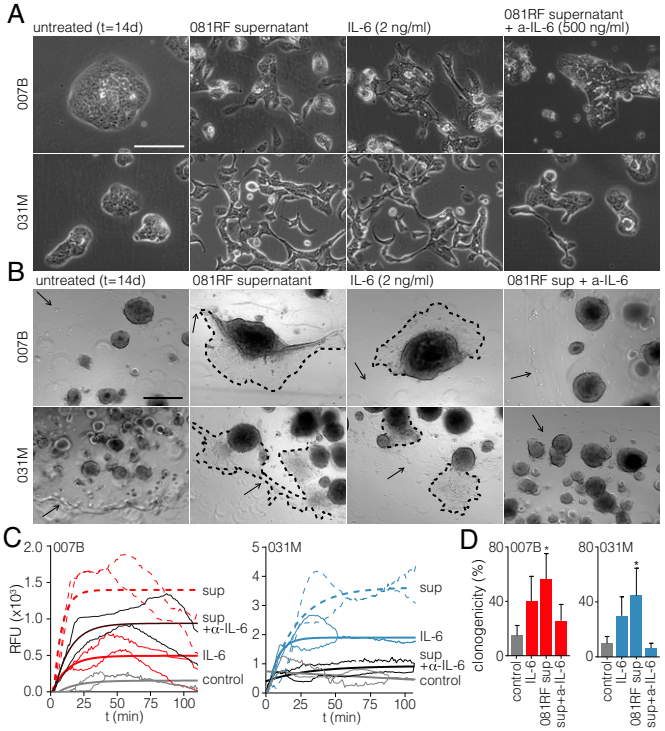

Fig. 3. CAF-secreted IL-6 induces epithelial-to-mesenchymal transition. (*A*) The 007B and 031M cultures were exposed to the following conditions for 14 d: unconditioned medium (untreated), 081RF supernatant (1 in 4 diluted), recombinant IL-6, and 081RF + IL-6–neutralizing antibody. Morphology was assessed by phase-contrast microscopy. (Scale bar: 200 μm.) (*B*) As for *A* using 007B and 031M organoid cultures. Dashed lines indicate the migratory front of cells migrating out of the organoid. Arrows indicate the edge of the Matrigel cushion. (*C*) Transwell migration assays on 007B and 031M cells cultured for 14 d in the conditions as for *A* before the assay. In the transwell assays, 1% FCS was used as a chemoattractant. Migration shown is corrected for no-attractant controls (medium without FCS), $n = 3$. *P* values were determined by two-way ANOVA and Tukey's multiple comparisons correction, one-phase exponential curves were fitted, and the lines of matching color indicate the SD. (*D*) Limiting dilution assays were performed using 007B and 031M cells after incubation for 14 d in the indicated conditions. Cells were sorted into 96-well plates. Bar graphs show means ± SEM, $n = 3$. $*P < 0.05$, $**P < 0.01$, $***P < 0.001$, and $****P < 0.0001$. Significance was tested by two-sided unpaired *t* tests compared with the control.

(Fig. 3 *C* and *D*). Furthermore, concomitant with the up-regulation of EMT markers, cancer stem cell (CSC) markers *CD44*/CD44, prominin-1 (*PROM1*/CD133), and leucine-rich repeat-containing G protein-coupled receptor 5 (*LGR5*/LGR5) were increased (*SI Appendix*, Fig. S9 *G–L*). This was accompanied by an increased clonogenicity in limiting dilution assays (Fig. 3*D*) and implies that stroma-derived IL-6 drives many of the EMT-associated biological programs that are known to contribute to poor outcome in cancer.

To allow an assessment of the contributions of IL-6 signaling to tumor growth in vivo, the problem of species incompatibility between IL-6 and its receptor needed to be addressed (33). To allow mouse-human transsignaling and human-human autocrine signaling, we generated 031M cells expressing the mouse IL-6 receptor (mIL-6Ra) and human IL-6 ligand (hIL-6; and empty vector), respectively. These cells were injected in immunodeficient mice, and tumor outgrowth was observed only from cells expressing mIL6Ra or hIL-6 (*SI Appendix*, Fig. S11), confirming that IL-6 signaling also contributes to clonogenicity in vivo.

Stroma-Derived IL-6 Confers Resistance to Radiochemotherapy in EAC Patients. In current clinical practice, patients diagnosed with EAC eligible for curative therapy receive neoadjuvant carboplatin, paclitaxel, and fractionated radiation [the CROSS regimen (3)]. To study whether CAF-derived IL-6 can confer resistance to such a triple-modality regimen, we modeled this treatment by determining the combined doses of the regimen components that allow for a near-complete cell killing, similar to the encouraging but often incomplete responses seen in patients. Primary EAC cells were given one dose of carboplatin and paclitaxel and subsequently received seven radiation doses of 1 Gy. Colony formation was assessed, and efficient outgrowth was observed only in the presence of IL-6 (Fig. 4 *A* and *B*). To confirm this response in a model system more representative of human disease, early-passage PDX-derived EAC organoids (which underwent clonal selection only during graft expansion, which ensured the tumor cell origin of the organoids) were subjected to the same treatment, and the ability to passage the cultures after triple-modality treatment was determined (Fig. 4*C*). Organoid outgrowth following passaging was observed only in cultures exposed to IL-6 and did not occur in the control or IL-6–neutralized conditions.

Having identified the molecule responsible for EMT-associated therapy resistance in EAC cells exposed to triple-modality treatments, a logical step would be to measure this cytokine in the serum of patients and correlate it to response, yielding a predictive marker that can predict neoadjuvant treatment outcome. Serum samples from 82 EAC patients before start of neoadjuvant chemoradiotherapy were analyzed for IL-6, and no significant difference was found between patients grouped by tumor response (Mandard score; Fig. 4*D*), probably reflecting the association of IL-6 with numerous inflammatory conditions. Instead, we identified ADAM12 by correlative gene expression analyses as a more specific marker for stromal CAFs (*SI Appendix*, Fig. S6*G*). Its expression was associated with poor prognosis (*SI Appendix*, Fig. S6*H*). ADAM12 levels in the serum are known to correlate with disease stage in lung cancer (34–36), and its expression is mostly confined to stromal cells in gastrointestinal cancers (37, 38). Measuring serum ADAM12 in these patients revealed a strong correlation to circulating IL-6 (Fig. 4*E*). Of note, high circulating ADAM12 levels significantly correlated with poor response to chemoradiation (Mandard score of 3–4) in EAC patients (Fig. 4*F*). Treatment of CAFs with recombinant IL-6 or blocking IL-6 ligand with antibody did not induce or affect ADAM12 secretion, but addition of recombinant TGF-β did (Fig. 4*G*). This confirms that ADAM12 is a feature of highly activated CAFs and that this activation likely does not result from autocrine IL-6 signaling. Future work will have to validate these findings in other cohorts and confirm whether ADAM12 is indeed an accurate measure of IL-6–producing CAFs in the activated EAC stroma and a predictive marker for currently applicable treatments against EAC.

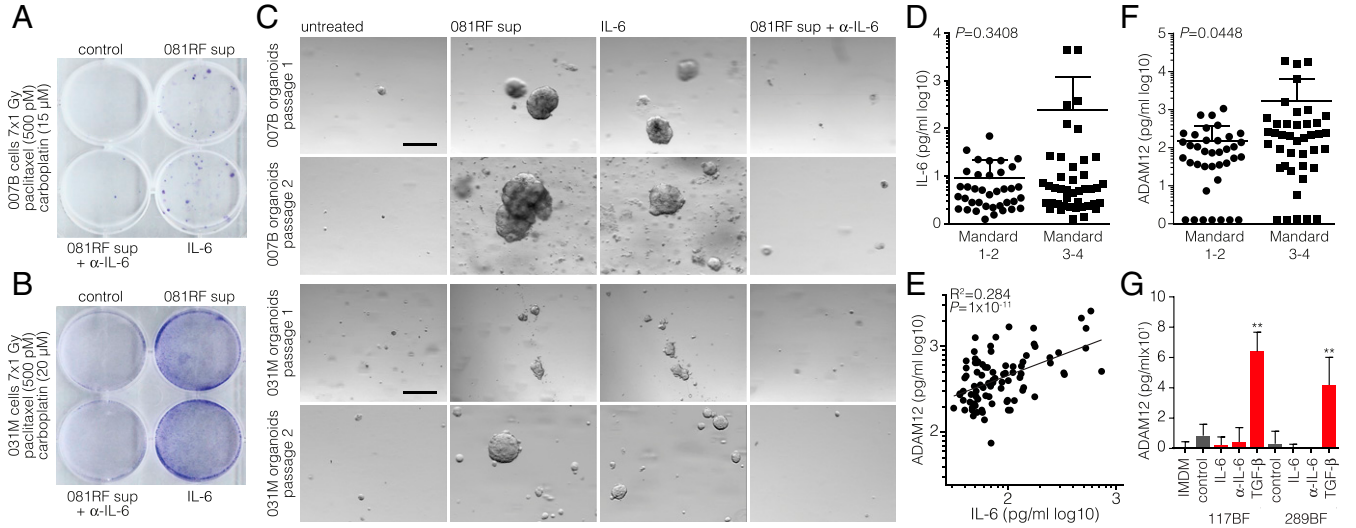

Fig. 4. Stroma-derived IL-6 confers resistance to radiochemotherapy in EAC patients. (*A*) Clonogenic assays were performed on 007B cells after receiving one dose of the indicated cytostatic agents and seven doses of 1-Gy radiation. Cells were cultured in the following conditions for 10 d before the assay: control, 081RF supernatant, 081RF supernatant + IL-6–neutralizing antibody (500 ng/mL), or recombinant IL-6 (2 ng/mL). (*B*) As for *A*, using 031M cells. (*C*) The 007B and 031M organoid cultures were exposed to conditions as for *A* and *B*. The culture conditions were maintained throughout the assay, and morphology was monitored by phase-contrast microscopy. Shown are passage 1 (4 wk after treatment) and passage 2 (10 d after passage 1). (Scale bar: 200 μm.) (*D*) Blood was drawn and processed for serum storage from pretreatment EAC patients seen at the Academic Medical Center (AMC) ($n = 80$). All patients then received the neoadjuvant CROSS regimen, and Mandard score was determined by a pathologist. IL-6 serum levels of pretreated EAC patients were measured using ELISA. (*E*) The same serum samples as for *D* were used to measure ADAM12. Correlation of serum IL-6 and ADAM12 levels was determined on all samples, including those with blank measurements. The log-scale plot excludes blanks. (*F*) As for *D*, showing ADAM12 serum levels. Graphs show means ± SD. Significance was tested by the Mann–Whitney *U* test. (*G*) Indicated CAF lines were treated with IL-6 (10 ng/mL), IL-6–neutralizing antibody (1 μg/mL), or TGF-β (5 ng/mL) for 3 d. Supernatant was harvested after an additional 7 d, and ADAM12 levels were analyzed by ELISA. $^{**}P < 0.01$.

Discussion

Despite the advent of multimodality treatment, the overall survival of EAC patients remains poor. This is mainly due to therapy resistance and aggressive tumor growth leading to the early onset of metastatic disease. Previous studies on therapy resistance mechanisms in EAC mostly focused on tumor cell-intrinsic mechanisms, but it is now well-established that the stroma plays a central role as well (8, 9, 26, 27). Here we investigated how EAC-associated fibroblasts impact therapy resistance and identified IL-6 as a mediator of this resistance.

Upon treatment with recombinant or CAF-derived IL-6, we observed that the tumor cells obtained a mesenchymal phenotype that was accompanied by increased migration. Indeed, EMT is associated with poor disease outcome, attributed to the enhanced migratory capacity of the cells that is thought to contribute to metastasis (39–41). Importantly, EMT was recently described to confer resistance to cytotoxic agents, which underscores our observation of EMT-induced chemoresistance (42, 43). In addition, IL-6 enhanced clonogenicity in vitro and in vivo and up-regulated the expression of CSC markers, which has been linked to EMT as well (44). This could well explain the resistance against a broad range of cytotoxic agents and radiation that has been attributed to stemlike cancer cells. Furthermore, IL-6 has previously been linked to tumor invasion and metastatic progression (45), and here we showed that this is, at least in part, caused by the induction of EMT.

The apparent readiness of EAC cells to undergo EMT in response to extrinsic cues and stresses offers a unique opportunity to study the kinetics of this transition. In doing so, we found that the onset of EMT in response to CAF supernatant already occurred within several days, explaining the resistance observed in the cell viability assays. Also, this rapid transition to a mesenchymal cell state is in line with the notion that therapy resistance is instructed by IL-6 in the majority of the EAC tumor cell population, rather than selection of a limited number of clones.

The ability to predict treatment response by means of a non-invasive serum marker would be of immense clinical value. IL-6 is primarily involved in inflammatory processes, and its serum levels are elevated in patients suffering from asthma and rheumatoid arthritis (46, 47). Furthermore, inflammation has a great influence on the onset and progression of various cancer types, including EAC (48–50). Consequently, IL-6 is likely not a very specific serum marker for treatment response in EAC, and we found no correlation with IL-6 serum levels and response to neoadjuvant treatment. Instead, we identified *ADAM12* as one of the stromal genes most strongly correlating with *IL6*. ADAM12 is known to exist in the circulation (51), and indeed, ADAM12 serum levels in pretreated EAC patients from our hospital differed significantly between patients dichotomized by response to neoadjuvant treatment. This suggests that the amount of "activated stroma" can be seen as a measure, or predictor, of therapy response. This could also be of use for specific stroma-targeting strategies, including the direct targeting of CAFs (52). However, considerable overlap exists in ADAM12 levels between the two groups, and for use in clinical decision making, additional markers should be included. Also, it should be noted that the stroma is not the only factor to impact therapy response and that other compartments and signals contribute to heterogeneous responses that therefore cannot be explained by serum-borne proxies of stromal activation status.

In summary, our data elucidate the mechanisms through which the tumor stroma contributes to therapy resistance in EAC and demonstrate that ADAM12 serum levels predict treatment outcome in patients. Given these findings and the availability of relevant FDA-approved IL-6–targeting agents, we propose that addition of such agents to currently applicable regimens should be strongly considered.

Materials and Methods

Informed Consent Procedure. Signed informed consent was obtained for all patients included in the BiOES biobank according to procedures approved by the Academic Medical Center's ethical committee (MEC 01/288#08.17.1042). This consent covers all procedures described in this paper, including the collection of clinical data, tissue, and blood for marker analysis and expansion as xenografts and in vitro cultures.

Establishment of Primary Cancer-Associated Fibroblasts. Primary EAC-associated fibroblasts were established from resected tumor specimens of EAC patients treated at the Academic Medical Center (Amsterdam, The Netherlands) according to the CROSS regimen (carboplatin, paclitaxel, and radiation) (3). Fresh tumor pieces were washed three times for 5 min with PBS containing penicillin (100 units/mL), streptomycin (500 μg/mL), and gentamicin (5 μg/mL); cut into small pieces; and resuspended in DMEM containing Liberase and DNase for 45 min. Subsequently, cells were resuspended, passed through a 100-μm cell strainer, and spun down. Cells were resuspended in IMDM medium containing 8% FBS, L-glutamine (2 mM), penicillin (100 units/mL), and streptomycin (500 μg/mL) and plated in a T25 culture flask. After 48 h, all nonadherent cells were discarded by washing with PBS. Cells were maintained according to standard culture conditions, and upon reaching 80% confluence, cell sorting by negative selection (EPCAM-negative) was performed to obtain a pure fibroblast culture. Antibodies are listed in *SI Appendix*, Table S1. The primary EAC-associated fibroblasts exposed to neoadjuvant chemoradiation used are as follows: AMC-EAC-081RF (081RF) and AMC-EAC-243RF (243RF). Treatment-naive primary fibroblasts are AMC-EAC-P117BF (117BF) and AMC-EAC-289BF (289BF).

Establishment of Primary Tumor Cell Cultures. Primary cultures were established as described before from PDXs (53). Briefly, tumor material of patients diagnosed with EAC in the Academic Medical Center (Amsterdam, The Netherlands) was obtained in accordance with approval by the institute's ethical committee (MEC 01/288#08.17.1042) (54). The tumor material was expanded in NOD.Cg-*Prkdc*^{scid} *Il2rg*^{tm1Wjl}/SzJ (NSG) immunodeficient mice. Ethical approval was obtained (LEX102774), and the NSG mice were bred and maintained at the local animal facility according to local legislation. Cultures were maintained in Advanced DMEM/F12 (Gibco) with 1:100 N2 (Invitrogen), 2 mM L-glutamine (Sigma-Aldrich), 5 mM Hepes (Life Technologies), 0.15% D-glucose (Sigma-Aldrich), 100 μM β-mercaptoethanol (Sigma-Aldrich), 10 μg/mL insulin (Sigma-Aldrich), 2 μg/mL heparin (Sigma-Aldrich), and 1:1,000 trace elements B and C (Fisher Scientific). The primary EAC cultures used are as follows: AMC-EAC-007B (007B), which was established from a pretreatment biopsy diagnosis, and AMC-EAC-031M (031M), established from a pretreatment biopsy of a liver metastasis of esophageal adenocarcinoma.

Immunofluorescence was performed as previously described (30). For cell culture and viability assay, flow cytometry, limiting dilution assays, migration assay, quantitative RT-PCR, survival, gene set enrichment analysis, and gene correlations (*SI Appendix, Supplementary Materials and Methods*).

Cytokine Array. The growth factor array AAH-CYT-4000 (RayBiotech) was performed according to the manufacturer's protocol using 081RF supernatant incubated for 3 d, with unconditioned supernatant as the control. Detection was carried out using a FuijFilm LAS4000, and spot intensity was quantified using Image J. Fold induction was calculated according to the manufacturer's instructions; each value was controlled for the positive control spots on each membrane and the values obtained from the unconditioned culture medium. The fold induction values represent the average of duplicate measurements from the membrane. For mouse-derived CAFs, the Mouse Cytokine Array C2000 (RayBiotech) was used. For IL-6 measurements on cell cultures, see *SI Appendix, Supplementary Materials and Methods*.

Western Blot. Western blots were performed as previously described (54). Following transfer, membranes were cut to allow detection of multiple antigens, guided by prestained molecular weight markers. See *SI Appendix*, Fig. S7 for full membranes and cutting strategy. Dashed boxes indicate crops shown in Fig. 2*I*. Primary antibodies (listed in *SI Appendix*, Table S1) were incubated overnight at 4 °C. Proteins were imaged using Lumi-Light plus Western blot substrate (Pierce, Thermo Scientific) on a FuijFilm LAS 4000 imager. In parallel to the ECL images, epi-illuminated photographs were captured to document membrane topology.

Organoid Cultures. Early-passage PDX-derived organoids (P1-10) were cultured in 24-well plates in drops of 50 μL Matrigel (Corning) and maintained in serum-free Advanced DMEM/F12 (Gibco), supplemented with N2 supplement (Invitrogen), 2 mM L-glutamine, 100 μM β-mercaptoethanol (Sigma), trace elements B and C (Fisher Scientific), 5 mM Hepes (Life Technologies), 2 μg/mL heparin (Sigma), 10 μg/mL insulin (Sigma), and 0.15% D-glucose (Sigma). For passaging, organoids and Matrigel were mechanically disrupted in unsupplemented Advanced DMEM/F12 medium (wash medium). The organoids were washed and resuspended two times before passaging. Different culture conditions as indicated were maintained during the assay; chemoradiation was given before passaging as indicated in Fig. 4. Medium was refreshed twice a week.

Clonogenic Assay. The 007B and 031M organoids cultured in either control medium, medium containing 25% 081RF supernatant, or 25% 081RF supernatant which was preincubated for 30 min with IL-6–neutralizing antibody were treated with paclitaxel and carboplatin at the indicated concentrations and irradiated (7× 1 Gy). After 2 wk, the organoids were replated in six-well plates at a density of 2,000 cells/well. Colony forming was determined after 4 wk, using crystal violet. During the assay, the culture medium was refreshed twice a week according to the conditions stated above.

Serum Marker Analysis. Serum from patients diagnosed with EAC in the Academic Medical Center (Amsterdam, The Netherlands) was collected and stored at −80 °C, as approved by the institute's ethical committee (MEC 01/288#08.17.1042). Informed consent was obtained from all included patients, and blood was drawn before the start of neoadjuvant treatment according to the CROSS regimen. The human IL-6 and human ADAM12 ELISA (both R&D Systems DuoSet) were performed according to the manufacturer's procedures.

Statistical Analysis. For cell viability curves, two-way ANOVA tests were used to determine statistical significance. For all of the other experiments, one-way ANOVA tests were performed, unless noted otherwise. *P* values and the *R* values of gene expression correlations were determined by linear regression analysis. For the survival analysis, statistical significance was determined using the log-rank (Mantel–Cox) test. For comparison of tumor take in mice, the χ^2 test was used. All statistical analyses were performed using GraphPad Prism 7. Error bars show the mean ± SEM. A P value of <0.05 was considered statistically significant.

ACKNOWLEDGMENTS. We thank A. E. Gerards and J. C. A. Colen-de Koning (Amsterdam UMC) for providing therapeutic monoclonal antibodies, R. A. Mulder-Jibodh and C. E. Daal (Amsterdam UMC) for technical assistance, and Dr. Vermeulen for fruitful discussion. This work was supported by a personal research grant from the Dutch Research Council to H.W.M.v.L (016.096.010) and Koningin Wilhelmina Fonds (KWF) Dutch Cancer Society Project Grant 10992/2017-1.

1. Pennathur A, Gibson MK, Jobe BA, Luketich JD (2013) Oesophageal carcinoma. *Lancet* 381:400–412.
2. Edgren G, Adami HO, Weiderpass E, Nyrén O (2013) A global assessment of the oesophageal adenocarcinoma epidemic. *Gut* 62:1406–1414, and erratum (2013) 62:1820.
3. Shapiro J, CROSS study group (2015) Neoadjuvant chemoradiotherapy plus surgery versus surgery alone for oesophageal or junctional cancer (CROSS): Long-term results of a randomised controlled trial. *Lancet Oncol* 16:1090–1098.
4. Sun Y (2015) Translational horizons in the tumor microenvironment: Harnessing breakthroughs and targeting cures. *Med Res Rev* 35:408–436.
5. Kalluri R, Zeisberg M (2006) Fibroblasts in cancer. *Nat Rev Cancer* 6:392–401.
6. Tsujino T, et al. (2007) Stromal myofibroblasts predict disease recurrence for colorectal cancer. *Clin Cancer Res* 13:2082–2090.
7. Yamashita M, et al. (2012) Role of stromal myofibroblasts in invasive breast cancer: Stromal expression of alpha-smooth muscle actin correlates with worse clinical outcome. *Breast Cancer* 19:170–176.
8. Schoppmann SF, et al. (2013) Podoplanin expressing cancer associated fibroblasts are associated with unfavourable prognosis in adenocarcinoma of the esophagus. *Clin Exp Metastasis* 30:441–446.
9. Underwood TJ, et al. (2015) Cancer-associated fibroblasts predict poor outcome and promote periostin-dependent invasion in oesophageal adenocarcinoma. *J Pathol* 235:466–477.
10. Hu M, Polyak K (2008) Microenvironmental regulation of cancer development. *Curr Opin Genet Dev* 18:27–34.
11. Rodier F, et al. (2009) Persistent DNA damage signalling triggers senescence-associated inflammatory cytokine secretion. *Nat Cell Biol* 11:973–979, and erratum (2009) 11:1272.
12. Yun UJ, Park SE, Jo YS, Kim J, Shin DY (2012) DNA damage induces the IL-6/STAT3 signaling pathway, which has anti-senescence and growth-promoting functions in human tumors. *Cancer Lett* 323:155–160.
13. Gao J, Zhao S, Halstensen TS (2016) Increased interleukin-6 expression is associated with poor prognosis and acquired cisplatin resistance in head and neck squamous cell carcinoma. *Oncol Rep* 35:3265–3274.
14. Karakasheva TA, et al. (2018) IL-6 mediates cross-talk between tumor cells and activated fibroblasts in the tumor microenvironment. *Cancer Res* 78:4957–4970.
15. Wu CT, Chen MF, Chen WC, Hsieh CC (2013) The role of IL-6 in the radiation response of prostate cancer. *Radiat Oncol* 8:159.
16. Xu M, et al. (2017) Interactions between interleukin-6 and myeloid-derived suppressor cells drive the chemoresistant phenotype of hepatocellular cancer. *Exp Cell Res* 351:142–149.
17. Hodge DR, et al. (2005) Interleukin 6 supports the maintenance of p53 tumor suppressor gene promoter methylation. *Cancer Res* 65:4673–4682.
18. Leu CM, Wong FH, Chang C, Huang SF, Hu CP (2003) Interleukin-6 acts as an anti-apoptotic factor in human esophageal carcinoma cells through the activation of both STAT3 and mitogen-activated protein kinase pathways. *Oncogene* 22:7809–7818.
19. Garcia-Tuñón I, et al. (2005) IL-6, its receptors and its relationship with bcl-2 and bax proteins in infiltrating and in situ human breast carcinoma. *Histopathology* 47:82–89.
20. Zhang F, et al. (2016) Cisplatin treatment increases stemness through upregulation of hypoxia-inducible factors by interleukin-6 in non-small cell lung cancer. *Cancer Sci* 107:746–754.
21. Huang WC, et al. (2016) Interleukin-6 expression contributes to lapatinib resistance through maintenance of stemness property in HER2-positive breast cancer cells. *Oncotarget* 7:62352–62363.
22. Helbig G, et al. (2003) NF-kappaB promotes breast cancer cell migration and metastasis by inducing the expression of the chemokine receptor CXCR4. *J Biol Chem* 278:21631–21638.
23. Yadav A, Kumar B, Datta J, Teknos TN, Kumar P (2011) IL-6 promotes head and neck tumor metastasis by inducing epithelial-mesenchymal transition via the JAK-STAT3-SNAIL signaling pathway. *Mol Cancer Res* 9:1658–1667.
24. Liu H, et al. (2015) Aberrantly expressed Fra-1 by IL-6/STAT3 transactivation promotes colorectal cancer aggressiveness through epithelial-mesenchymal transition. *Carcinogenesis* 36:459–468.
25. Saadi A, et al. (2010) Stromal genes discriminate preinvasive from invasive disease, predict outcome, and highlight inflammatory pathways in digestive cancers. *Proc Natl Acad Sci USA* 107:2177–2182.
26. Jomrich G, et al. (2014) Stromal expression of carbonic anhydrase IX in esophageal cancer. *Clin Transl Oncol* 16:966–972.
27. Courrech Staal EF, et al. (2011) Reproducibility and validation of tumour stroma ratio scoring on oesophageal adenocarcinoma biopsies. *Eur J Cancer* 47:375–382.
28. Cancer Genome Atlas Research Network (2017) Integrated genomic characterization of oesophageal carcinoma. *Nature* 541:169–175.
29. Krause L, et al. (2016) Identification of the CIMP-like subtype and aberrant methylation of members of the chromosomal segregation and spindle assembly pathways in esophageal adenocarcinoma. *Carcinogenesis* 37:356–365.
30. Ebbing EA, et al. (2017) Esophageal adenocarcinoma cells and xenograft tumors exposed to Erb-b2 receptor tyrosine kinase 2 and 3 inhibitors activate transforming growth factor beta signaling, which induces epithelial to mesenchymal transition. *Gastroenterology* 153:63–76.e14.
31. Biddle A, et al. (2011) Cancer stem cells in squamous cell carcinoma switch between two distinct phenotypes that are preferentially migratory or proliferative. *Cancer Res* 71:5317–5326.
32. Pádua Alves C, et al. (2013) Brief report: The lincRNA Hotair is required for epithelial-to-mesenchymal transition and stemness maintenance of cancer cell lines. *Stem Cells* 31:2827–2832.
33. Hammacher A, et al. (1994) Structure-function analysis of human IL-6: Identification of two distinct regions that are important for receptor binding. *Protein Sci* 3:2280–2293.
34. Roy R, Wewer UM, Zurakowski D, Pories SE, Moses MA (2004) ADAM 12 cleaves extracellular matrix proteins and correlates with cancer status and stage. *J Biol Chem* 279:51323–51330.
35. Rocks N, et al. (2006) Expression of a disintegrin and metalloprotease (ADAM and ADAMTS) enzymes in human non-small-cell lung carcinomas (NSCLC). *Br J Cancer* 94:724–730.
36. Shao S, et al. (2014) ADAM-12 as a diagnostic marker for the proliferation, migration and invasion in patients with small cell lung cancer. *PLoS One* 9:e85936.
37. Yu J, et al. (2012) Unlike pancreatic cancer cells pancreatic cancer associated fibroblasts display minimal gene induction after 5-aza-2′-deoxycytidine. *PLoS One* 7:e43456.
38. Veenstra VL, et al. (2018) ADAM12 is a circulating marker for stromal activation in pancreatic cancer and predicts response to chemotherapy. *Oncogenesis* 7:87.
39. Shioiri M, et al. (2006) Slug expression is an independent prognostic parameter for poor survival in colorectal carcinoma patients. *Br J Cancer* 94:1816–1822.
40. Spaderna S, et al. (2006) A transient, EMT-linked loss of basement membranes indicates metastasis and poor survival in colorectal cancer. *Gastroenterology* 131:830–840.
41. Hur K, et al. (2013) MicroRNA-200c modulates epithelial-to-mesenchymal transition (EMT) in human colorectal cancer metastasis. *Gut* 62:1315–1326.
42. Fischer KR, et al. (2015) Epithelial-to-mesenchymal transition is not required for lung metastasis but contributes to chemoresistance. *Nature* 527:472–476.
43. Zheng X, et al. (2015) Epithelial-to-mesenchymal transition is dispensable for metastasis but induces chemoresistance in pancreatic cancer. *Nature* 527:525–530.
44. Mani SA, et al. (2008) The epithelial-mesenchymal transition generates cells with properties of stem cells. *Cell* 133:704–715.
45. Kumari N, Dwarakanath BS, Das A, Bhatt AN (2016) Role of interleukin-6 in cancer progression and therapeutic resistance. *Tumour Biol* 37:11553–11572.
46. Yokoyama A, et al. (1995) Circulating interleukin-6 levels in patients with bronchial asthma. *Am J Respir Crit Care Med* 151:1354–1358.
47. Burska A, Boissinot M, Ponchel F (2014) Cytokines as biomarkers in rheumatoid arthritis. *Mediators Inflamm* 2014:545493.
48. Rubenstein JH, Shaheen NJ (2015) Epidemiology, diagnosis, and management of esophageal adenocarcinoma. *Gastroenterology* 149:302–317.e1.
49. Fitzgerald RC, et al. (2002) Inflammatory gradient in Barrett's oesophagus: Implications for disease complications. *Gut* 51:316–322.
50. O'Riordan JM, et al. (2005) Proinflammatory cytokine and nuclear factor kappa-B expression along the inflammation-metaplasia-dysplasia-adenocarcinoma sequence in the esophagus. *Am J Gastroenterol* 100:1257–1264.
51. Gilpin BJ, et al. (1998) A novel, secreted form of human ADAM 12 (meltrin alpha) provokes myogenesis in vivo. *J Biol Chem* 273:157–166.
52. Hanley CJ, et al. (2018) Targeting the myofibroblastic cancer-associated fibroblast phenotype through inhibition of NOX4. *J Natl Cancer Inst* 110:109–120.
53. Damhofer H, et al. (2015) Establishment of patient-derived xenograft models and cell lines for malignancies of the upper gastrointestinal tract. *J Transl Med* 13:115.
54. Ebbing EA, et al. (2016) ADAM10-mediated release of heregulin confers resistance to trastuzumab by activating HER3. *Oncotarget* 7:10243–10254.